Jeremy Walker graduated in spring 2020 from Weber State University. He earned his degree *magna cum laude* with departmental honors in physics. In the summer of 2019, he conducted research at the University of Memphis in the Research Experience for Undergraduates program funded by the National Science Foundation. Jeremy has done two research projects in computational physics and presented one project at the American Physical Society's Four Corners meeting in 2018. He has been accepted to a master's program in applied physics at the University of Oregon.

Jeremy Walker

A Molecular Dynamics Study of Lipid Membranes Cushioned by Polymer Brushes

Faculty Sponsor

Dr. Mohammed Lardji

Abstract

We present a numerical study of self-assembled lipid membranes, that are cushioned by polymer brushes, using molecular dynamics simulations of a coarse-grained implicit solvent model.

Introduction

Lipid bilayers are a crucial component of life. When a group of lipids is exposed to water, the hydrophobic groups turn toward each other while the hydrophilic groups turn toward the water. These bilayers make up the ever-important lipid membrane of cells. The lipid membrane acts as a barrier between the inner and outer parts of the cell, provides structural integrity for the cell, and supports numerous large transmembrane proteins needed for proper cellular function. Without lipid membranes, cells would spill out of their bounds and not even simple single celled organisms could survive.

Prior studies have employed a variety of techniques to study the function, structure, and dynamics of lipid bilayers. At the most basic level, substrate supported studies can be done (McCabe, 2013; Andersson, 2016; Deverall, 2005). In these experiments, the membrane is placed directly on a substrate with a water layer cushion that is a few nanometers thick. This limits the motion of the membrane in the direction perpendicular to the substrate and is an especially poor way to study transmembrane proteins because they are too large and often denature with excessive contact with the substrate due to their protrusion below the bilayer (McCabe, 2013). To overcome these obstacles, an additional layer of polymer can be added below the membrane to act as a cushion. This polymer supported model allows transmembrane proteins to sink into the polymer and as such, they are less likely to denature. One type of polymer support is a polymer brush, which is formed by chemically tethering polymer chains to a substrate and introducing a membrane on the free ends. In this computational study, we will simulate a polymer brush support because it mimics the cytoskeleton of the cell and as such, is a better model to study biological processes. We aim to study the mutual effects of the membrane and the polymer brush interactions and to increase the theoretical understanding of this model for use in future experiments.

Model And Computational Method

A coarse-grained implicit-solvent model was used (Revalee, 2008; Laraji, 2016), in which a lipid molecule is coarse-grained into a semi-flexible chain composed of one head (h) bead and two tail (t) beads. The potential energy of the lipid bilayer has three contributions:

$$U(\{r_i\}) = \sum U_0^{\alpha_i \alpha_j}(r_{ij}) + \sum_{(i,j)} U_{bond}(r_{ij}) + \sum_{(i,j,k)} U_{bend}(\vec{r}_i, \vec{r}_j, \vec{r}_k), \quad (1)$$

where $\vec{r}_i$ describes the coordinates of bead i, $r_{ij} = |\vec{r}_i - \vec{r}_j|$, and $\alpha_i (= h \text{ or } t)$ is the type of bead i. In Eq. (1), $U_0^{\alpha\beta}$ is a soft two-body potential, between beads of types α and β and separated by a distance r, and is a piece-wise function given by (Laradji, 2016),

$$U_0^{\alpha\beta}(r) = \begin{cases} (U_{max}^{\alpha\beta} - U_{min}^{\alpha\beta}) \dfrac{(r_m - r)^2}{r_m^2} + U_{min}^{\alpha\beta} & \text{if } r \le r_m \\ -2U_{min}^{\alpha\beta} \dfrac{(r_c - r)^3}{(r_c - r_m)^3} + 3U_{min}^{\alpha\beta} \dfrac{(r_c - r)^2}{(r_c - r_m)^3} & \text{if } r < r \le r_c \\ 0 & \text{if } r > r_c, \end{cases} \quad (2)$$

where $U_{max}^{\alpha\beta} > 0$ and $U_{min}^{\alpha\beta} \le 0$ for any pair (α, β). $U_{min}^{\alpha\beta} = 0$ implies a fully repulsive interaction between beads α and β, and $U_{min}^{\alpha\beta} < 0$ implies a short-range attraction between the two beads. The self-assembly of the lipids into thermodynamically stable bilayers is ensured by choosing $U_{min}^{hh} = U_{min}^{ht} = 0$ and a sufficiently negative value of U_{min}^{tt} (Laradji, 2016).

In Eq. (1), U_{bond} ensures connectivity between beads that belong to the same lipid chain and is given by

$$U_{\text{bond}}(r) = \frac{k_{\text{bond}}}{2}(r - a_b)^2, \quad (3)$$

where k_{bond} is the bond stiness coefficient and a_b is the preferred bond length. Finally, U_{bend} in Eq. (1) is a three-body potential that provides bending stiness to the lipid chains and is given by

$$U_{\text{bend}}(\vec{r}_{i-1}, \vec{r}_i, \vec{r}_{i+1}) = \frac{k_{\text{bend}}}{2} \left(\cos\varphi_0 - \frac{\vec{r}_{i,i-1} \cdot \vec{r}_{i,i+1}}{r_{i,i-1}\, r_{i,i+1}} \right)^2 \quad (4)$$

where k_{bend} is the bending stiness coefficient and φ_0 is the preferred splay angle of the lipid chain, taken to be 180°.

All beads are moved using a molecular dynamics scheme with a Langevin thermostat (Grest, 1986),

$$\dot{\vec{r}}_i(t) = \vec{v}_i(t) \tag{5}$$

$$m_i \dot{\vec{v}}_i(t) = -\nabla_i U(\{\vec{r}_i\}) - \Gamma \vec{v}_i(t) + \sigma \vec{\Xi}_i(t), \tag{6}$$

where m_i is the mass of bead i and Γ is a bead's friction coefficient. $\sigma\vec{\Xi}_i(t)$ is a random force with zero mean, and is uncorrelated for dierent particles, dierent times, and dierent components. Γ and σ are inter-related through the fluctuation-dissipation theorem leading to $\Gamma = \sigma^2 = 2k_BT$.

The simulations are performed in the *NVT* ensemble, where N is the total number of beads in the system. The model interaction parameters are given by,

$$\begin{aligned}
U^{hh}_{max} &= U^{ht}_{max} = 100\epsilon, \\
U^{tt}_{max} &= 200\epsilon, \\
U^{hh}_{min} &= U^{ht}_{min} = 0, \\
U^{tt}_{min} &= -6\epsilon, \\
U^{mm}_{max} &= xyz, \\
U^{mm}_{min} &= 0, \\
U^{mh}_{max} &= 1210\epsilon / r_m^2, \\
U^{mt}_{min} &= 0, \\
U^{mh}_{min} &= -\mathcal{E}, \\
^{k}bond &= 100\epsilon / r_m^2, \\
^{k}bend &= 100\epsilon, \\
r_c &= 2r_m, \\
a_b &= 0.7r_m.
\end{aligned} \tag{7}$$

In Eq. (7), $\mathcal{E}$ is the adhesion energy of a lipid head group per unit of area of the NP, and is henceforth used to define the *adhesion strength*.

All simulations are performed at $k_BT = 3.0\epsilon$, with a time step $\Delta t = 0.02\tau$, where $\tau = r_m (m/\epsilon)^{1/2}$. Eqs. (5) and (6) are integrated using the velocity-Verlet algorithm.

The bending modulus of the bare bilayer, with the interaction parameters given by Eq. (7), as extracted from the spectrum of the LM height fluctuations, is $\kappa \approx 30 k_BT$ (Laradji, 2016), which is comparable to that of DPPC in the fluid phase (Nagle, 2015). The length scale, r_m, is estimated from comparing the value of the thickness of the LM ~ $5r_m$, typical to phospholipid bilayer. We therefore estimate $r_m \approx 1$ nm. Hence, in the remainder of this article, all lengths are expressed in nanometers, and the adhesion strength, $\mathcal{E}$, is expressed in k_BT/nm^2.

Results

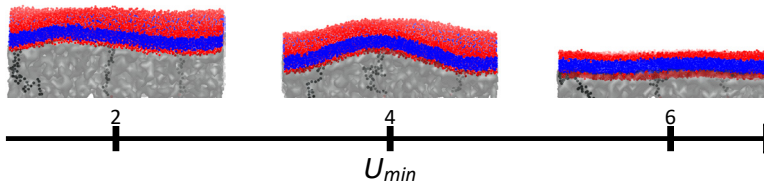

Figure 1. Typical configurations of the membrane for increasing $\mathcal{E}$. This system has a chain length N = 50, and a polymer brush grafting density σ = 0.1. Clearly, as $\mathcal{E}$ is increased, the average height of both the membrane and the polymer brush decrease. Note that between $\mathcal{E}$ = 2 and $\mathcal{E}$ = 4, the membrane fluctuations increased. The opposite occurred for $\mathcal{E}$ values past 4. Individual polymer chains have been highlighted to show how a typical chain behaves in the brush.

As shown in Fig. 1, the average height of the membrane and polymer brush decreases with increasing $\mathcal{E}$. Because of this compression, the density of the polymer layer is expected to increase. When a density profile is taken along the z-axis, the density of the polymer brush does indeed increase. However, this increase is largely localized near the membrane while the lower levels of the brush remain unchanged, as shown in Fig. 2. From this we conclude that a relatively highly dense layer of monomers forms directly under the bilayer. The increase in $\mathcal{E}$ favors an increase in the amount of contact between the lipid head groups and the monomers, which can only be achieved by

having the membrane move closer to the substrate.

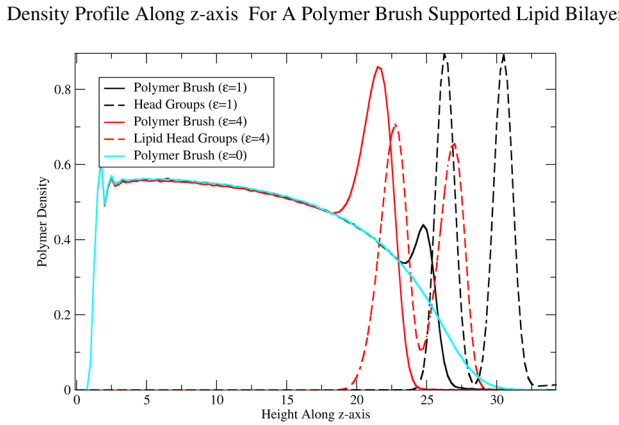

Figure 2. The density of the polymer brush is changed in the presence of a membrane. $\mathcal{E} = 0$ corresponds to a polymer brush that does not interact attractively with a membrane. With attraction to the lipid heads in the membrane, the polymer brush density increases near the lipid heads. However, the density of the lower levels is relatively unchanged. Additionally, the shortening and widening of the peaks associated with the lipid head groups when $\mathcal{E} = 4$ again imply the fluctuations of the membrane have increased as seen in Fig. 1. This data was collected from a system with $N = 50$ and $\sigma = 0.25$

Next, the bilayer's structure can first be characterized by the width of its fluctuations, $w = \sqrt{h^2 - (\bar{h})^2}$ where we define h as the height (z-coordinate) of a lipid head group in the top leaflet of the membrane. Fig. 3 and 4 demonstrate changes in the structure of the membrane caused by varying the grafting density or length of the polymer chains. There are three main features in Figs. 3 and 4. Namely, for very low $\mathcal{E}$, the membrane is not absorbed; followed by an abrupt decay in w at the absorption transition. For intermediate values of $\mathcal{E}$, there is an increase in the width, w. It then reaches a peak and then decreases for even higher $\mathcal{E}$. Because we expected a monotonic decrease in the fluctuations in the membrane, the intermediate increase of w vs. $\mathcal{E}$ is puzzling and needs further investigation. In contrast, the decrease of w vs. $\mathcal{E}$ for high $\mathcal{E}$ is expected. The non-monotonous behavior of w vs. $\mathcal{E}$ should be the result of some structural dierence of the top layer of the polymer brush (vicinal to the bilayer).

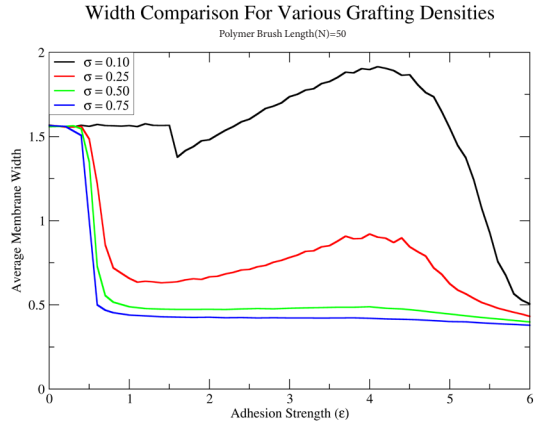

Figure 3. There is a systematic relationship between the width of w and the grafting density of the polymer brush, σ. For increasing σ, the membrane becomes more rigid and the membrane absorbs earlier for more dense systems. Surprisingly, for low density systems, the bilayer has more fluctuations than a free membrane. The non-monotonic behavior becomes less pronounced as σ is increased. This data was collected with $N = 50$.

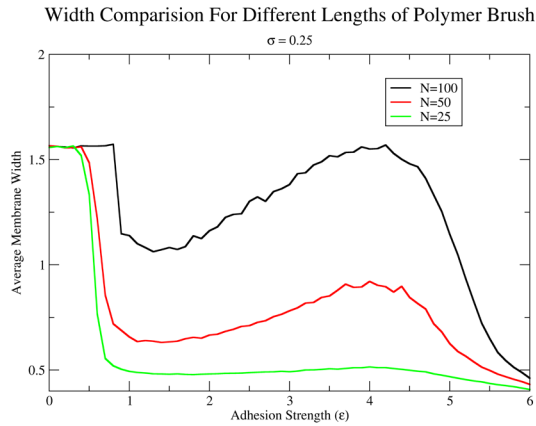

Figure 4. There is a systematic relationship between w and the number of monomers per polymer chain, N. For decreasing N, the membrane becomes more rigid and the membrane absorbs earlier for shorter systems.

The structure factor of a free membrane is given by,

$$S(q) = \frac{k_B T}{\gamma q^2 + \kappa q^4 + \cdots} \tag{8}$$

where γ is the tension coefficient and κ is the bending modulus of the membrane. We can use this structure factor to further investigate how the membrane changes when absorbed onto a polymer brush. Transforming the structure factor to $1/q^2 S(q)$ vs. q^2 allows us to see the contributions of each term in the denominator. Figure 5 shows that for small wavevectors, $1/q^2 S(q)$ actually intercepts the y-axis at a finite value, which increases with increasing $\mathcal{E}$. This is expected as the absorption of the bilayer on the polymer brush leads to an energy cost resulting from vertical translation of the bilayer.

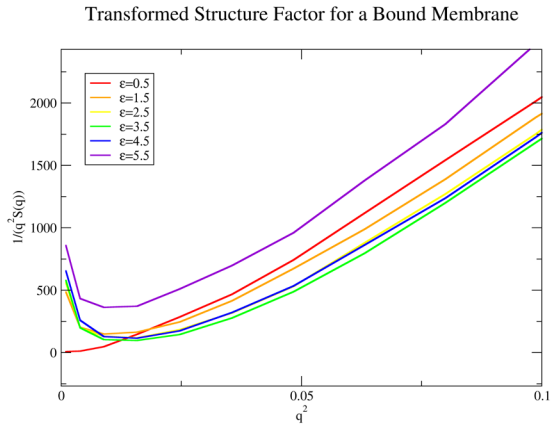

Figure 5. A plot of $1 / q^2 S(q)$ vs. q^2 transformed from Eq.(8) Note that for an unbound membrane ($\mathcal{E} = 0.5$) the plot converges to zero as expected in the case of a tensionless membrane. However, when the bilayer is adsorbed on the brush, $1 / q^2 S(q)$ increases rapidly as $q \to 0$. This indicates that due to binding, the bilayer has a preferred position along the z-axis, leading to the emergence of a mass term in the effective Hamiltonian of the bilayer. Interestingly, for small q (long wavelengths), $1 / q^2 S(q)$ has a non-monotonic behavior, namely it decreases with increasing $\mathcal{E}$, then increases. This behavior mirrors that of w shown above.

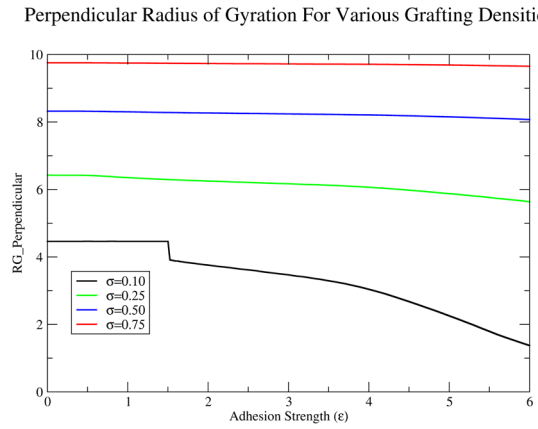

Figure 6. $R_\perp$ monotonously decreases with increasing $\mathcal{E}$. This is expected since the monomers which are within the adhesion sublayer below the bilayer only weakly contribute to $R_\perp$, and the bilayer gets closer to the substrate as $\mathcal{E}$ increases (hence $R_\perp$ decreases with increasing $\mathcal{E}$). This is to say that the behavior of $R_\perp$ is not surprising and not that interesting (in the sense that it does not help in understanding the non-monotonic behavior of w vs. $\mathcal{E}$).

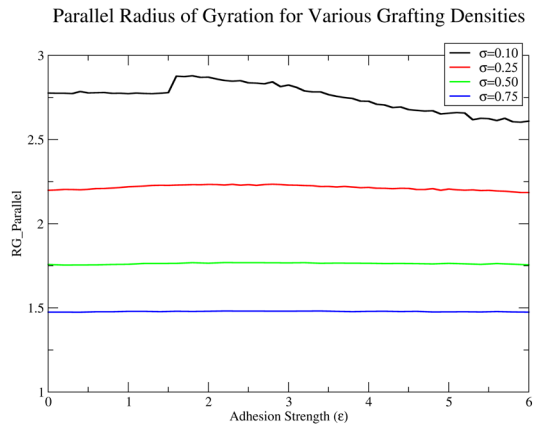

Figure 7. The radius of gyration acquired by summing the radius of gyration along both the x and y axes in quadrature. While the effect is small, there is a non-monotonic trend here that peaks around $\mathcal{E} = 2$. This is due to the binding of the top monomers to the membrane.

In order to understand the non-monotonic behavior of w vs. $\mathcal{E}$, we observed the radius of gyration along the $z-$axis ($R_{\perp}$) and the $xy-$plane ($R_{\parallel}$) to provide more information about the structure of the polymer brush. As shown in Fig. 6, $R_{\perp}$ was not useful in analyzing the non-monotonic behavior of interest. In contrast, Fig. 7 shows that $R_{\parallel}$ has a more interesting non-monotonic behavior, though the change is very weak.

Next, we can look at the contact energy, $E_{contact}$ that results from the interaction of monomers with lipid head groups. From Fig. 2, it is expected that $E_{contact}$ will not depend on the length of the polymer chains, N.

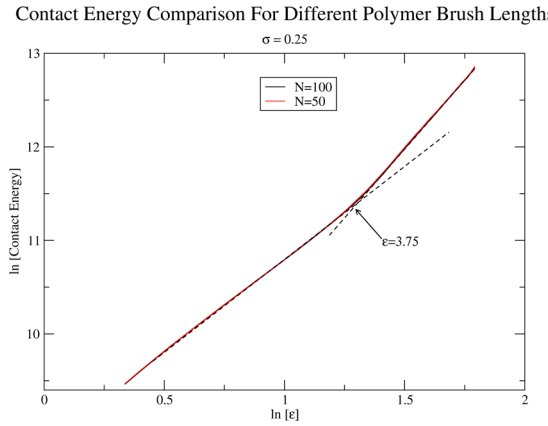

Figure 8. A ln-ln plot of the contact energy between the monomers in the polymer chain and the lipid head groups on the underside of the membrane. $N = 25$ and $N = 50$ chain lengths were used. The contact energy plots lay over top one another, showing that the lower levels of the polymer brush do not participate in the interaction with the membrane. E_{contact} steadily increases with $\mathcal{E}$. However, this increase becomes more pronounced for $\mathcal{E}$ larger than 3.75. This corresponds closely to the peak seen in Figs. 3 and 4.

Figure 8 implies that the non-monotonic behavior of the fluctuations of the membrane is the result of different structural modes of the polymer brush. For low values of the interaction strength between the polymer monomers and the bilayer, the free energy of the system is dominated by the conformational entropy of the portion of the polymer in the vicinity of the bilayer rather than by interactions. The reverse occurs for high values of $\mathcal{E}$. The polymers conformational entropy is higher for low grafting densities than large ones. Hence, the effect above is expected to be stronger for low

values of σ. The non-monotonic behavior of w is indeed more pronounced for low values of σ, as shown in Fig 3.

Conclusions

Overall findings show clear mutual interactions between the lipid membrane and polymer brush. These effects vary with adhesion strength.

For intermediate adhesion strength ($\mathcal{E} \lessapprox 4$), membrane fluctuations increase with adhesion strength. This trend is dominated by the polymer's conformational entropy. This effect is increased with increasing polymer length or decreasing grafting density.

For large adhesion strength ($\mathcal{E} \lessapprox 4$), the membrane fluctuations decrease with increasing adhesion strength. In this region the trend is dominated by the adhesion interaction between the membrane and the polymers.

The fluctuations of the membrane are reduced by either increasing the grafting density or decreasing the length of the polymer brush.

The greatest change in the polymer brush occurs near the membrane. The polymer brush becomes denser directly beneath the membrane as more monomers bind to it. This is evident in the peak occurring in the density profile near the membrane, the small change in the parallel radius of gyration, and the contact energy's independence of brush length. When supported by a polymer brush, the properties of lipid membranes change observably

Because of the clear changes in both the properties of the polymer brush and the lipid membrane, a slightly different model may be presented in the future to help preserve the properties of the lipid membrane in the presence of the brush. All the data here is presented with the assumption that the membrane was tensionless before its adhesion on the membrane. If this assumption is found to be false, the new model will need to change, so the membrane is tensionless in the beginning.

The theoretical understanding acquired from this study is meant to be a launching pad for future experimental work. Using the computational model described here, researchers can learn how their membranes will change if they use a polymer brush support without spending money and time producing the actual polymer brush. If the theoretical results match the desired conditions, an experiment can be conducted with more confidence.

References

Andersson, J., & Köper, I. (2016). Tethered and Polymer Supported Bilayer Lipid Membranes: Structure and Function. *Membranes*, *6*(2), 30. doi: 10.3390/membranes6020030

Deverall, M., Gindl, E., Sinner, E.-K., Besir, H., Ruehe, J., Saxton, M., & Naumann, C. (2005). Membrane Lateral Mobility Obstructed by Polymer-Tethered Lipids Studied at the Single Molecule Level. *Biophysical Journal*, *88*(3), 1875–1886. doi: 10.1529/biophysj.104.050559

Grest, G. S., & Kremer, K. (1986). Molecular dynamics simulation for polymers in the presence of a heat bath. *Physical Review A*, *33*(5), 3628–3631. doi: 10.1103/physreva.33.3628

Laradji, M., & Kumar, P. B. S. (2016). Preface for the special issue "Biomembranes." *International Journal of Advances in Engineering Sciences and Applied Mathematics*, *8*(2), 87–87. doi: 10.1007/s12572-016-0167-0

Mccabe, I. P., & Forstner, M. B. (2013). Polymer Supported Lipid Bilayers. *Open Journal of Biophysics*, *03*(01), 59–69. doi: 10.4236/ojbiphy.2013.31a008

Revalee, J. D., Laradji, M., & Kumar, P. B. S. (2008). Implicit-solvent mesoscale model based on soft-core potentials for self-assembled lipid membranes. *The Journal of Chemical Physics*, *128*(3), 035102. doi: 10.1063/1.2825300